Technical University of Denmark

DTU

Hard, charged spheres in spherical pores. Grand canonical ensemble Monte Carlo calculations

Sloth, Peter; Sørensen, T. S.

DTU Library
Technical Information Center of Denmark

Hard, charged spheres in spherical pores. Grand canonical ensemble Monte Carlo calculations

P. Sloth and T. S. Sørensen
Fysisk-Kemisk Institut, Technical University of Denmark, Bldg. 206, DK 2800 Lyngby, Denmark

A model consisting of hard charged spheres inside hard spherical pores is investigated by grand canonical ensemble Monte Carlo calculations. It is found that the mean ionic density profiles in the pores are almost the same when the wall of the pore is moderately charged as when it is uncharged. Also, a bulklike phase is found to be present at the center of the pores in surprisingly small systems. Finally, the Poisson–Boltzman approximation is discussed in the light of our Monte Carlo results.

I. INTRODUCTION

The properties of inhomogeneous ionic systems are of wide spread practical and theoretical interest. In this work, we investigate a statistical mechanical model of mobile ions in a dielectric continuum, confined in a hard spherical pore. The most obvious application of such a model would be to a spherical pore in a porous medium. Alternatively, the pore might, e.g., represent a simple model of a water droplet in a water-in-oil microemulsion (i.e., the interior of a reverse micelle),[1] or a water droplet in air. In passing, it should be mentioned, that a few studies of more sophisticated models for reverse micelles have already been made.[2,3]

The present model, which is described in more detail in Sec. II, is studied by grand canonical ensemble Monte Carlo (GCEMC) calculations.[4] This implies that the pore is able to exchange particles with a remote bulk system. In Sec. III, a description of the GCEMC method is given, and numerical results are presented in Sec. IV. As an interesting by-product, our results indicate that a bulklike phase is formed at moderate ionic concentrations in surprisingly small systems, if we disregard the part of the system close to the boundary. Finally, we compare the MC results with the Poisson–Boltzmann (PB) approximation in Sec. V. This is of considerable interest, because the PB equation is often applied to actual electrochemical problems, although its validity is not always known *a priori*.

II. THE MODEL

We consider a primitive model electrolyte solution inside a spherical pore with hard walls. The pore may be charged. In that case, the charge is assumed to be uniformly distributed on the surface of the wall of the pore. For the sake of simplicity, we furthermore assume that the particles inside the pore do not interact directly with particles outside the pore. That is, we consider only an isolated pore. A similarly simple model for the interactions between two neutral reverse micelles has recently been studied by canonical ensemble MC calculations.[5]

The interionic interactions are modelled by the primitive model of electrolyte solutions (i.e., hard charged spheres in a dielectric continuum), which is specified by the pair potential function between a particle i at $\mathbf{r}_i$ and a particle j at $\mathbf{r}_j$ ($\mathbf{r}_{ij} = \mathbf{r}_j - \mathbf{r}_i$)

$$u_{ij}(\mathbf{r}_{ij}) = \begin{cases} \infty, & |\mathbf{r}_{ij}| < (d_i + d_j)/2, \\ q_i q_j/4\pi\epsilon|\mathbf{r}_{ij}|, & |\mathbf{r}_{ij}| \geqslant (d_i + d_j)/2. \end{cases} \quad (2.1)$$

In Eq. (2.1), q_i and d_i are the charge and the diameter of ion no i, respectively, and ϵ is the dielectric permitivity. It should be noted that any effects of a nonuniform dielectric permitivity are not taken into account in the present simple model. The cavity of radius R is introduced by the single particle potential function

$$u_i(\mathbf{r}_i) = \begin{cases} q_i\Psi^*, & |\mathbf{r}_i| \leqslant R - d_i/2, \\ \infty, & |\mathbf{r}_i| > R - d_i/2, \end{cases} \quad (2.2)$$

where

$$\Psi^* = Q/4\pi\epsilon R \quad (2.3)$$

is the (constant) contribution to the electric potential in the pore, set up by a total charge Q uniformly distributed on the pore wall. In Eq. (2.2), the positions $\mathbf{r}_i$ are taken relatively to the center of the pore. By Eq. (2.3), it is assumed that no other external contribution to the electrostatic potential in the pore is present.

The ions inside the pore are assumed to be in equilibrium with a homogeneous bulk fase. That is, the particles may in principle "jump" in and out of the pore.

Let ρ_α^b be the bulk density of species α, and let $\langle N_\alpha \rangle$ be the average number of particles of species α in the pore. The average density $\langle \rho_\alpha \rangle$ of particles of species α inside the pore can then be given by

$$\langle \rho_\alpha \rangle = 3\langle N_\alpha \rangle/4\pi R^3 = K_\alpha \rho_\alpha^b, \quad (2.4)$$

where K_α is a partition coefficient. In the ideal case, K_α reduces to a "Henry law" constant $K_{\alpha 0}$, with the value

$$K_{\alpha 0} = (1 - d_\alpha/2R)^3. \quad (2.5)$$

The average electrostatic potential $\Psi(\mathbf{r})$ at the position $\mathbf{r}$ in the pore is given as a solution to Poissons equation

$$\nabla^2\Psi(\mathbf{r}) = -\rho_q(\mathbf{r})/\epsilon \quad (2.6a)$$

with $\rho_q(\mathbf{r}) = \Sigma_\alpha q_\alpha \rho_\alpha(\mathbf{r})$. Here, $\rho_q(\mathbf{r})$ is the average charge density distribution and $\rho_\alpha(\mathbf{r})$ is the average local density of species α. For the spherical pore, studied here, we find the following solution to Eq. (2.6a): ($r \equiv |\mathbf{r}|$)

$$\epsilon\Psi(r) = \frac{1}{r}\int_0^r t^2\rho_q(t)dt + \int_r^R t\rho_q(t)dt + \epsilon\Psi^*, \quad (2.6b)$$

where the last term is the contribution from the fixed charge of the pore wall.

III. GCEMC CALCULATIONS

We consider a two-component system with fixed volume (V) and absolute temperature (T). The system contains a mixture of cations and anions (denoted $+$ and $-$, respectively), and the electro chemical potentials, $\bar{\mu}_+$ and $\bar{\mu}_-$ are held fixed. The system may be considered to consist of Ω uniformly distributed sites, at which the ions can be centered. Let x_i denote a given configuration i of the system; let N_i^+ and N_i^- be the number of cations and anions, respectively, in this configuration, and let $U(x_i)$ be the corresponding *total* potential energy. The probability u_i of configuration x_i in the grand canonical ensemble is then given by

$$u_i = \frac{(\Delta V)^{N_i^+ + N_i^-}}{(\lambda_+^{N_i^+} \lambda_-^{N_i^-})^3}$$
$$\times \frac{\exp\{\beta [\bar{\mu}_+ N_i^+ + \bar{\mu}_- N_i^- - U(x_i)]\}}{\Xi(V,T,\bar{\mu}_+,\bar{\mu}_-)} \quad (3.1)$$

with

$$\Delta V = V/\Omega. \quad (3.2)$$

In Eq. (3.1), $\Xi(V,T,\bar{\mu}_+,\bar{\mu}_-)$ is the grand canonical partition function and $\lambda_\alpha \equiv [h^2\beta/2\pi m_\alpha]^{1/2}$ is the thermal deBroglie wavelength of species α (h being the Planck's constant, and m_α being the mass of a particle of species α). We have also introduced $\beta \equiv 1/k_B T$ where k_B is the Boltzmann constant. By Eq. (3.1) it is assumed that the particles are unlabeled. That is particles of the same kind are indistinguishable. We note that this formula is the discrete version of the usual classical statistical mechanical equation.

Equation (3.1) is used in a Markov chain[6] where the individual steps are generated such that a given configuration x_i occurs with a probability proportional to u_i as the length of the chain goes to infinity. Let p_{ij} be the one-step probability of going from configuration x_i to configuration x_j. Here, we require that the p_{ij}'s satisfies microscopic reversibility, i.e.,

$$u_i p_{ij} = u_j p_{ji} \quad (3.3)$$

with the normalizing condition

$$\Sigma_j p_{ij} = 1. \quad (3.4)$$

Let s_{ij} be the probability of *attempting* a transition from configuration x_i to configuration x_j ($i \neq j$), and let f_{ij} be the probability that this attempted move is accepted. Then $p_{ij} = s_{ij}f_{ij}$, and we may write Eq. (3.3) as

$$f_{ij}/f_{ji} = u_j s_{ji}/u_i s_{ij}. \quad (3.5)$$

The generation of a new configuration from a former could be performed in a number of ways, as long as the resulting procedure is ergodic. That is, the probability of transition between two *permissible* states via a finite number of steps in the Markovchain should be finite. In our program, one of the following four trial moves were attempted with equal probability:

(1) Addition of a cation at a randomly chosen position.
(2) Addition of an anion at a randomly chosen position.
(3) Removal of a randomly chosen cation.
(4) Removal of a randomly chosen anion.

Let us suppose that configuration x_i has N_i^α particles of species α and N_i^γ particles of species γ, and that configuration x_j has $N_j^\alpha = N_i^\alpha + 1$ particles of species α and $N_j^\gamma = N_i^\gamma$ particles of species γ ($\alpha \neq \gamma$). (The position of the $N_i^\alpha + N_i^\gamma$ particles being the same in both of the configuration.) In this case s_{ij} and s_{ji} are given by

$$s_{ij} = 1/4\Omega, \quad (3.6)$$

$$s_{ji} = 1/4N_j^\alpha = 1/4(N_i^\alpha + 1). \quad (3.7)$$

Combination of Eqs. (3.1) and (3.5)–(3.7) gives

$$f_{ij}/f_{ji} = \frac{V\exp(\beta\bar{\mu}_\alpha)}{N_j^\alpha \lambda_\alpha^3} \exp\{-\beta[U(x_j) - U(x_i)]\}. \quad (3.8)$$

The electrochemical potentials are determined by a homogeneous bulk phase with electrical potential Ψ^b. That is

$$\exp(\beta\bar{\mu}_\alpha)/\lambda_\alpha^3 = z_\alpha \exp(\beta q_\alpha \Psi^b), \quad (3.9)$$

where z_α is the activity of species α in the bulk fase.

Combination of Eqs. (3.8), (3.9), and (2.2) finally yields

$$f_{ij}/f_{ji} = \frac{V\exp[-\beta q_\alpha(\Psi^* - \Psi^b)]}{N_j^\alpha}$$
$$\times z_\alpha \exp\{-\beta[U^*(x_j) - U^*(x_i)]\}$$
$$\equiv F(i,j), \quad (3.10)$$

where U^* is the contribution to U given by a sum of *pair* potentials only. That is, U^* is a function which is independent of any applied electrical potential. In this work, we set $\Psi^b = 0$ by convention, i.e., we set $\Psi^* - \Psi^b = Q/4\pi\epsilon R$ —in accordance with Eq. (2.3).

Equation (3.8) was used in our program by setting the following acceptance probabilities:

$$f_{ij} = \min\{1, F(i,j)\} \quad \text{for addition,} \quad (3.11)$$

$$f_{ji} = \min\{1, 1/F(i,j)\} \quad \text{for deletion} \quad (3.12)$$

of a particle. This is the procedure commonly applied.

IV. RESULTS

In this section, we present numerical results for the restricted primitive model (RPM), in which the cations and anions have equal diameters $d_+ = d_- = a$, and are of charge q and $-q$, respectively. The RPM systems studied are specified by a Bjerrum parameter $B \equiv \beta |q_+ q_-|/4\pi\epsilon a = 1.681$ and two different values for the mean ionic activities, i.e., $z_\pm^* \equiv z_\pm a^3 = 0.015\,17$ and $z_\pm^* = 0.040\,85$. These parameters correspond to aqueous (bulk) 1:1-electrolyte solutions at 25 °C with molar salt concentrations $c_s \simeq 0.425$ mol/dm^3 and $c_s \simeq 1.00$ mol/dm^3, with $a = 4.25$ Å. The relation between the activities and the concentrations in the bulk are here estimated by application of the HNC approximation.[7] Whenever it is needed in the following treatment, we shall use the HNC values for the bulk densities.

GCEMC calculations were performed for a number of pores with radii between $R = 1.5a$ and $R = 9a$, and with

TABLE I. Grand canonical Monte Carlo results for $z_{\pm}^* = 0.015\ 17$ and $B = 1.681$.

R/a	Q/e_0	No. of config $\times 10^{-6}$	$\langle N_+ \rangle$	$\langle N_- \rangle$	K_+^*	K_-^*	$a^3 \langle \rho_\pm \rangle_c{}^*$
1.5	0	10	0.0637_8		0.775		
	1	15	0.0237_5	0.170_3	0.289	2.069	
2.0	0	10	0.232_9		0.838		
	1	15	0.132_9	0.412_8	0.478	1.486	
2.5	0	30	0.584		0.887		0.0183
	1	15	0.418_4	0.820_4	0.635	1.246	0.0185
3.5	0	20	2.08_5		0.938		0.0193
	1	15	1.81_8	2.38_6	0.818	1.074	0.0193
5.0	0	20	7.22_7		0.964		0.0195
	1	20	6.88_5	7.58_3	0.918	1.011	0.0195
7.0	0	20	22.0_9		0.977		0.0196
	1	30	21.6_9	22.4_7	0.960	0.994	0.0196
9.0	0	30	49.7_3		0.984		0.0196
	1	50	49.2_7	50.1_1	0.975	0.991	0.0196

* $\langle \rho_\pm \rangle_c$ is the average density in the sphere given by $0 < r < R - 2a$.

$Q = 0$ and $Q = e_0$ (e_0 being the charge of a proton). The results for the average numbers of particles in the pores, as well as the reduced partition coefficients defined by $K_\alpha^* \equiv K_\alpha / K_{\alpha 0}$ are given in Tables I and II. Furthermore, the average mean ionic densities at the center of the pores are also given—these quantities will be discussed later on. The "mean ionic" reduced partition coefficients $K^* = \sqrt{K_+^* K_-^*}$ are shown in Fig. 1 as a function of $1/\tau$ [$\tau \equiv (R/a) - 0.5$]. From Fig. 1, it is seen that the K^* curves for $Q = 0$ and $Q = e_0$ are almost coinciding, especially at the lower density and/or at the lower values of $1/\tau$. Also, the values of K^* are less than one (in most cases) in contrast to (uncharged) hard sphere systems where $K^* \geqslant 1$.[8] [At the higher density, the computed values of K^* is slightly higher than unity for the largest pores. This finding might, however, be an artifact, if the HNC value for the bulk density is slightly too low.] The excess number of anions,

$\langle N_- \rangle - \langle N_+ \rangle$, obtained from the runs with $Q = e_0$, are plotted against $1/\tau$ in Fig. 2. It is seen that $\langle N_- \rangle - \langle N_+ \rangle$ approach unity as the pore become large. This correspond to the situation in which the *total* average charge of the pore becomes zero. It is noted, however, that the small pores deviate considerable from overall electroneutrality, especially at low ionic density. Here we emphasize that this finding applies for an isolated pore. If, e.g., a large number of identical pores are present in a system—with no ions in between the pores to shield the electrostatic interactions—the overall average charge of the individual pores should approach zero as the system tends to be infinitely large.

Some representative results for the reduced density profiles $G_\alpha(r) \equiv \rho_\alpha(r)/\rho_\alpha^b$ are shown in Figs. 3 and 4. In these Figs., the reduced mean ionic local density $G_\pm(r)$ is given by

$$G_\pm(r) = [G_+(r) G_-(r)]^{1/2}. \tag{4.1}$$

TABLE II. Grand canonical Monte Carlo results for $z_{\pm}^* = 0.040\ 85$ and $B = 1.681$.

| R/a	Q/e_0	No. of config $\times 10^{-6}$	$\langle N_+ \rangle$	$\langle N_- \rangle$	K_+^*	K_-^*	$a^3 \langle \rho_\pm \rangle_c{}^*$
1.5	0	20	0.169		0.873		-
	1	20	0.0722_6	0.380_4	0.373	1.964	-
2.0	0	10	0.623_7		0.954		-
	1	20	0.424_3	0.900_6	0.649	1.378	-
2.5	0	40	1.52_1		0.982		0.0461
	1	40	1.25_3	1.83_6	0.809	1.185	0.0460
3.5	0	15	5.21_1		0.996		0.0463
	1	25	4.87_6	5.57_9	0.932	1.067	0.0463
5.0	0	20	17.6_8		1.002		0.0463
	1	40	17.2_8	18.0_8	0.979	1.024	0.0463
7.0	0	25	53.3_9		1.004		0.0463
	1	42	52.9_4	53.8_0	0.995	1.011	0.0463
9.0	0	30	119.3_0		1.003		0.0463
	1	50	119.0_1	119.9_0	1.001	1.008	0.0464

* See footnote to Table I.
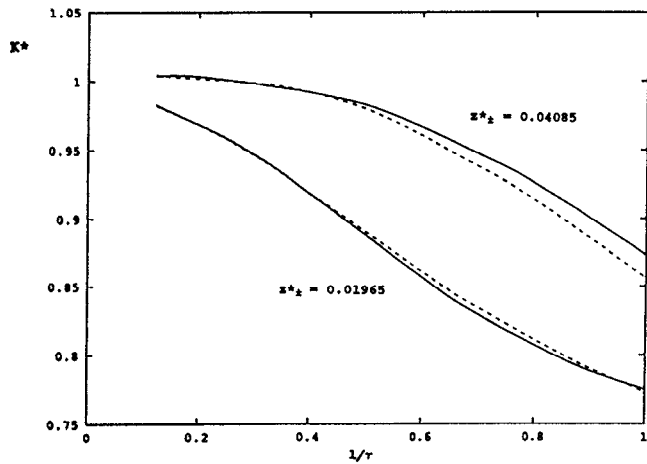
FIG. 1. Reduced mean ionic partition coefficients $K^* = \sqrt{K_+^* K_-^*}$ as a function of $1/\tau$. $Q = 0$ (—); $Q = e_0$ (---).

It is seen that $G_{\pm}$ (r), like K^*, is almost independent of Q in the present examples. When R/a is small, the G_+ (r) and G_- (r) curves for the charged pores are well separated for all values of r/a. As R/a increases, the reduced densities approach each other, having a value close to unity, except in the neighborhood of the pore wall, indicating that a bulklike phase is emerging at the center of the pores. In the case of the lower density, it is apparent that $G_\alpha(r) < 1$ near the pore wall if the pore is not too small. This is in contrast to hard-sphere systems where particles tend to pile up at the wall.[8] A likely physical explanation for this behavior is that the electrostatic shielding of the ions becomes less efficient near the wall.

Electric potential profiles, calculated by Eq. (2.6b) are shown by the solid lines in Figs. 5 and 6. For the large pores, we do only display $\Psi(r)$ close to the wall. This is because the correct form of the curves, in these cases, is masked by the considerable statistical noise at the centre of the pores. A more detailed discussion of Figs. 5 and 6 will be given in the next section.

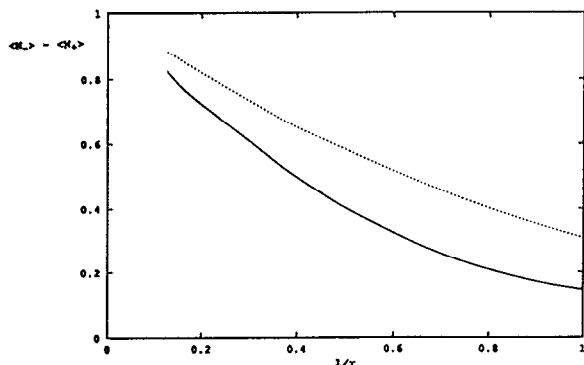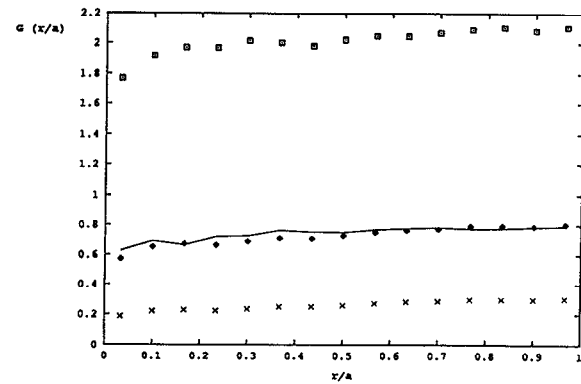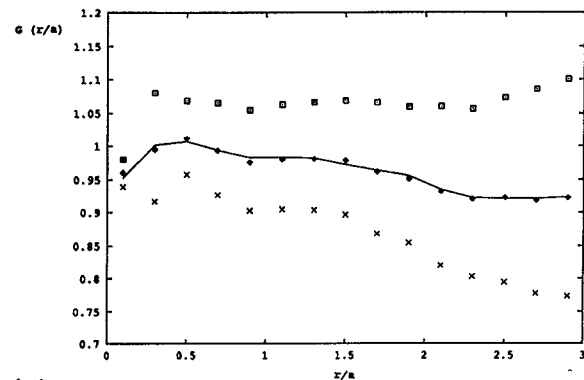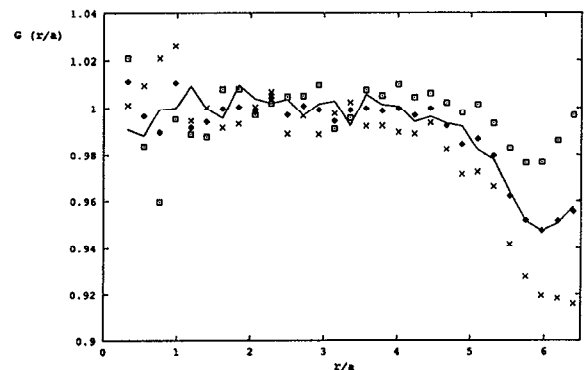From Figs. 3 and 4, it is seen that the density profiles inside the large pores are almost constant for $r < R - 2a$. We

FIG. 2. Excess number of anions $\langle N_- \rangle - \langle N_+ \rangle$ as a function of $1/\tau$. $z_{\pm}^* = 0.015\,17$ (—); $z_{\pm}^* = 0.040\,85$ (---).
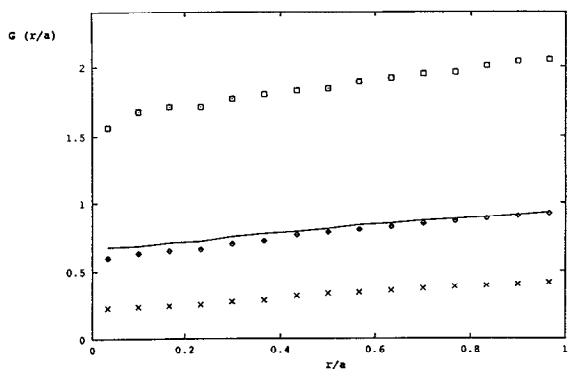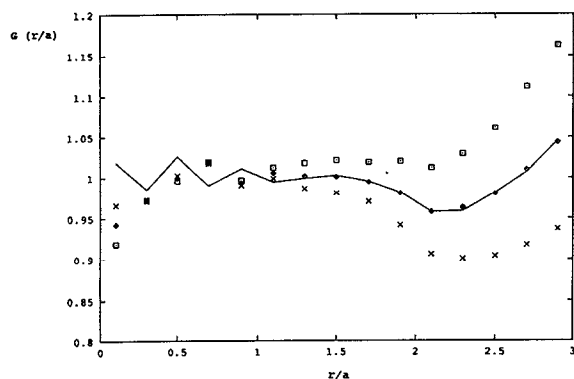

FIG. 3. Reduced density profiles for systems with $z_{\pm}^* = 0.015\,17$ and $B = 1.681$. $Q = 0$: $G_{\pm}$ $(r) = G_+$ $(r) = G_-$ (r) (—); $Q = e_0$: G_- (r) ($\square$), G_+ (r) ($\times$), $G_{\pm}$ (r) ($\Diamond$). (a) $R/a = 1.5$; (b) $R/a = 3.5$; (c) $R/a = 7$.

have calculated the average mean ionic densities at the centre of the larger pores. That is, the average density in the sphere given by $0 < r < R - 2a$. The results are given in the last columns of Tables I and II. For comparison the densities of the corresponding bulk systems estimated from the HNC approximation are $\rho_{\pm}^{*b} \equiv \rho_{\pm}^b a^3 = 0.0196_5$ and $\rho_{\pm}^{*b} = 0.0462_4$, respectively.[7] It is seen that the mean ionic density at the centre of the pores becomes almost constant if the pore is not too small, and the calculated densities are in satisfactory agreement with the HNC results for the bulk phase. This suggest that the application of *finite*, spherical systems may be an efficient method of calculating the relation between densities and chemical potentials in *bulk phases*
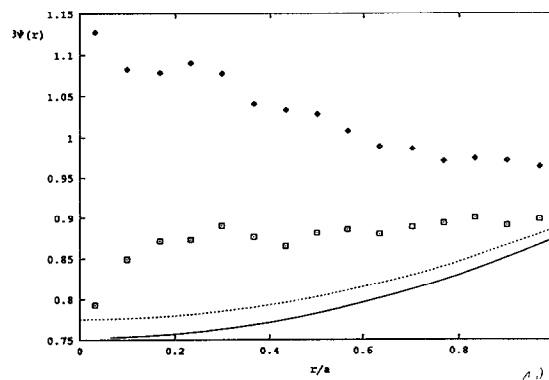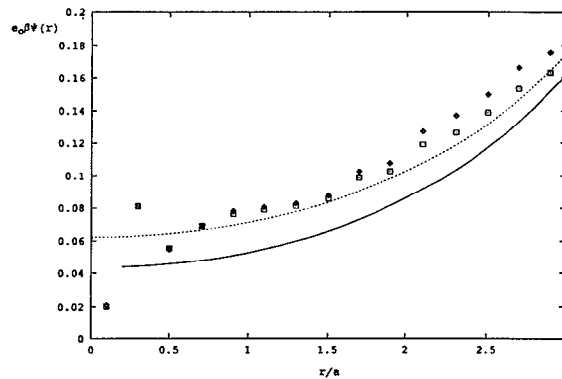
(a)

(b)
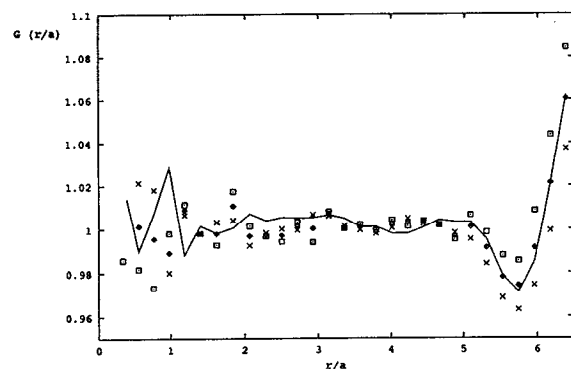
(c)

FIG. 4. Reduced density profiles for systems with $z_{\pm}^* = 0.040\,85$ and $B = 1.681$. Symbols are as in Fig. 3. (a) $R/a = 1.5$; (b) $R/a = 3.5$; (c) $R/a = 7$.

(a)

(b)

(c)

FIG. 5. Reduced electric potentials profiles for systems with $z_{\pm}^* = 0.015\,17$, $B = 1.681$ and $Q = e_0$. Integrated from charge density distributions (—); PB assumption: $\ln \sqrt{G_-(r)/G_+(r)}$ ($\Diamond$); l PB assumption: $[G_-(r) - G_+(r)]/2$ ($\Box$); l PB approximation Eq. (5.11) (- - -). (a) $R/a = 1.5$; (b) $R/a = 3.5$; (c) $R/a = 7$.
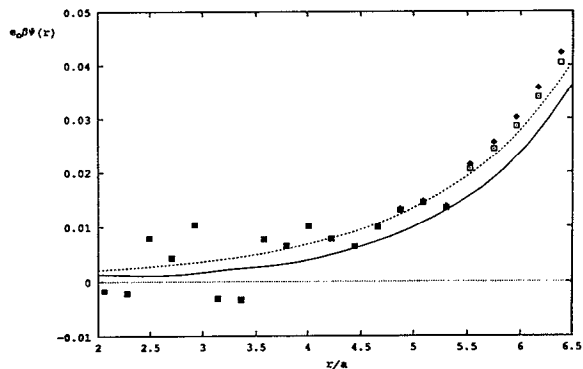
by GCEMC calculations, as long as the contributions from the "double layer" at the boundary of the system is neglected. Indeed, the estimated densities for the most dense systems, studied here, becomes independent of the size of the system (within the uncertainty of the calculations) for systems with a total number of particles as low as ca. 10–11 in the average. This is an interesting finding, because it has previously been generally accepted, that it is essential to use periodic boundary conditions, for systems of computational manageable sizes, to obtain realistic results for ionic bulk phases.

V. ON THE VALIDITY OF THE PB APPROXIMATION

The Poisson–Boltzmann (PB) approximation has been widely used in the field of electrochemistry. The PB approximation was first used many years ago in the Gouy–Chapman theory for the plane diffuse double layer,[9] and some 10 years later applied to spherical symmetry by Debye and Hückel in their famous theory for bulk electrolyte solutions.[10] The solution of the PB approximation for electrolytes inside a sphere has recently been discussed by different au-
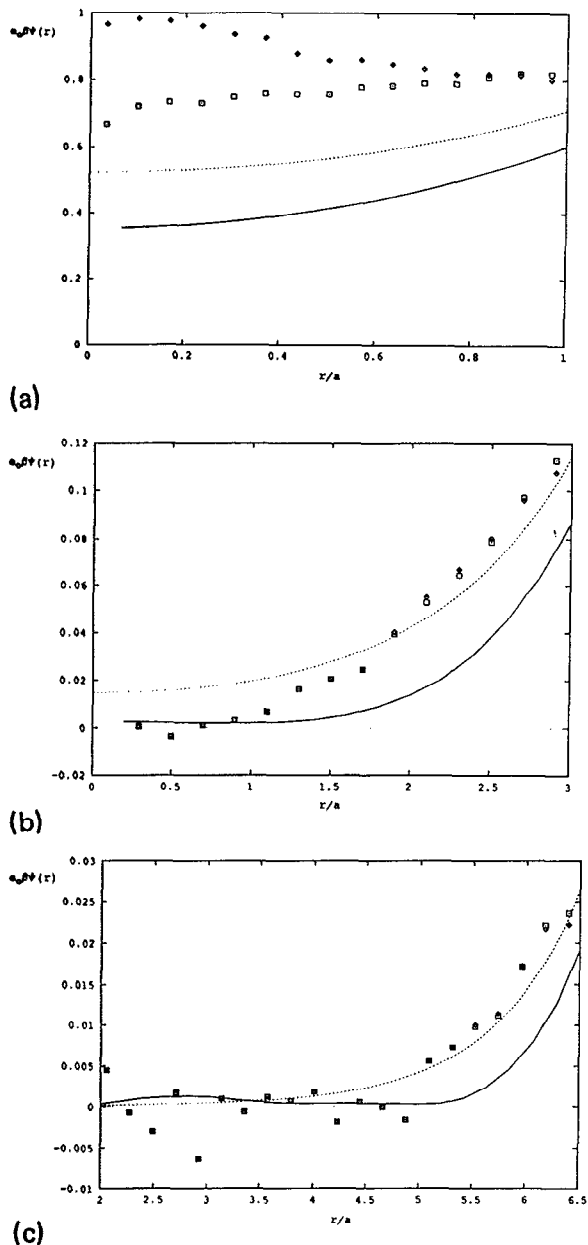
FIG. 6. Reduced electric potentials profiles for systems with $z^*_+ = 0.040\ 85$, $B = 1.681$, and $Q = e_0$. Symbols are as in Fig. 5. (a) $R/a = 1.5$; (b) $R/a = 3.5$; (c) $R/a = 7$.

thors.[1,11,12] In this section, we investigate the validity of the PB approximation in this case, by a direct comparison of the underlying assumptions with our Monte Carlo results.

A somewhat heuristic derivation of the PB equation might be the following: Let $z_\alpha(r)$ be a local activity of species α inside the pore. The condition for electrochemical equilibrium, may then be given by

$$\ln[z_\alpha(r)/z_\alpha] = \beta q_\alpha[\Psi^b - \Psi(r)]$$

or

$$\rho_\alpha(r) = \rho_\alpha^b[y_\alpha^b/y_\alpha(r)]\exp[-\beta q_\alpha\Delta\Psi(r)] \quad (5.1)$$

with

$$\Delta\Psi(r) \equiv \Psi(r) - \Psi^b, \quad (5.2)$$

where y_α^b and $y_\alpha(r)$ are the activity coefficients of species α

in the bulk and at a point r in the pore, respectively. It is noted that, strictly speaking, Eq. (5.1) is nothing but a defining equation for the quantity $y_\alpha(r)$. In the PB approximation, Eq. (5.1) is used together with the Poisson Eq. (2.6a), with the assumption $y_\alpha^b = y_\alpha(r)$. That is

$$\rho_\alpha^{PB}(r) = \rho_\alpha^b\exp[-\beta q_\alpha\Delta\Psi(r)], \quad (5.3)$$

where $\Delta\Psi(r)$ is determined by

$$\nabla^2(\Delta\Psi(r)) = -(1/\epsilon)\Sigma_\alpha\rho_\alpha^b q_\alpha\exp[-q_\alpha\beta\Delta\Psi(r)]. \quad (5.4)$$

This approximation intuitively appears to be reasonable if the concentrations in the neighbourhood of r do not deviate too much from the bulk density.

Equation (5.3) implies that $\rho_\pm(r) = \rho_\pm^b$ which is not a very good approximation, as can be seen from Figs. 3 and 4. However, it was found that $\rho_\pm(r)$ is quite independent of the charge of the pore wall, which suggests that one might obtain an improved approximation by writing

$$\rho_\alpha(r) \simeq \rho_\alpha(r;\Delta\Psi = 0)\exp[-\beta q_\alpha\Delta\Psi(r)], \quad (5.5)$$

where $\rho_\alpha(r;\Delta\Psi = 0)$ is the density profile in the corresponding pore with $\Delta\Psi = 0$, i.e., with $Q = 0$. For a charge symmetrical electrolyte ($q_+ = -q_- = q$) both of the Eqs. (5.3) and (5.5) yields

$$\ln\sqrt{\rho_+(r)/\rho_-(r)} = -\beta q\Delta\Psi(r). \quad (5.6)$$

As indicated before, we expect the PB approximation to be most reliable if $\rho_\alpha(r)/\rho_\alpha^b$ is close to unity. In this case the left-hand side of Eq. (5.6) might be approximated by

$$\ln\sqrt{\rho_+(r)/\rho_-(r)} \simeq (1/2)[\rho_+(r) - \rho_-(r)]/\rho_\pm^b$$

$$= (1/2)\rho_q(r)/(q\rho_\pm^b). \quad (5.7)$$

Combination of Eqs. (5.6) and (5.7) yields

$$\rho_q(r) \simeq -2\rho_\pm^b q^2\beta\Delta\Psi(r). \quad (5.8)$$

From Eqs. (5.8) and (2.6a) one obtains the linearized PB (lPB) equation:

$$\nabla^2\Psi(r) = \kappa^2\Delta\Psi(r) \quad (5.9)$$

with

$$\kappa^2 = 2\beta q^2\rho_\pm^b/\epsilon, \quad (5.10)$$

where κ is the inverse "Debye–Hückel screening length" for a charge-symmetrical electrolyte.

Equation (5.9) is readily solved for the present geometry. By setting $\Psi^b = 0$, in accordance with the previous discussion, we obtain the result

$$\Psi^{lPB}(r) = \Psi(0)\frac{\sinh(\kappa r)}{\kappa r}, \quad r/a \leqslant \tau, \quad (5.11)$$

where $\Psi(0)$ can be determined by application of Eqs. (5.8), (2.6b), and (5.10)

$$\Psi(0) = \frac{\Psi^*}{\cosh[\kappa(R - a/2)]}. \quad (5.12)$$

In Figs. 5 and 6, we show some representative MC results for $\ln\sqrt{\rho_-(r)/\rho_+(r)}$, $[\rho_-(r) - \rho_+(r)]/(2\rho_\pm^b)$ and $e_0\beta\Psi(r)$. For comparison are also given $\beta e_0\Psi(r)$ obtained from the analytical lPB expression Eq. (5.11). In the case of the small pores, it is seen that the PB assumption Eq.

(5.6), as well as the linearization given by Eq. (5.7) both are poor approximations. For the smallest pore (which also correspond to the largest applied electric potential) Eq. (5.6) is not even qualitatively correct. Figures 5 and 6 shows that the PB Eq. (5.6) is best, yet not excellent, for the large pores and at the low density. Furthermore, the linearization approximation given by Eq. (5.7) is seen to be very good in these cases.

[1] Y. Zhou and G. Stell, Mol. Phys. **68**, 1265 (1989).

[2] D. Brown and J. H. R. Clarke, J. Phys. Chem. **92**, 2881 (1988).

[3] P. Linse, J. Chem. Phys. **90**, 4992 (1989).

[4] D. J. Adams, Mol. Phys. **28**, 1241 (1974).

[5] A. Luzar and D. Bratko, J. Chem. Phys. **92**, 642 (1990).

[6] W. Feller, *An Introduction to Probability Theory and Its Applications* (Wiley, New York, 1950).

[7] P. Sloth and T. S. Sørensen, J. Phys. Chem. **94**, 2116 (1990).

[8] P. Sloth, J. Chem. Phys. **93**, 1292 (1990).

[9] G. Gouy, J. Phys. 9, 457 (1910); D. L. Chapman, Philos. Mag. **25**, 475 (1913).

[10] P. Debye and E. Hückel, Phys. Z. **24**, 742 (1923).

[11] D. J. Mitchell and B. W. Ninham, Langmuir **5**, 1121 (1989).

[12] G. A. van Aken, H. N. W. Lekkerkerker, J. Th. G. Overbeek, and P. L. de Bruyn, J. Phys. Chem. **94**, 8468 (1990).